SLAC-PUB-7388
October 1996

Analysis And Application Of Manifold Radiation In DDS 1: First Experiences[1]

R.M. Jones[†‡], N.M. Kroll[†‡], M. Seidel[†],C. Adolphsen[†], K.L.F. Bane[†], W.R. Fowkes[†], K. Ko[†], R.H. Miller[†], R.D. Ruth[†], and J.W. Wang[†]

†*Stanford Linear Accelerator Center, Stanford University, Stanford, CA 94309*
‡ *University of California, San Diego, La Jolla, CA 92093-0319*

Abstract

The cells in the SLAC DDS are designed in such a way that the transverse modes excited by the beam are detuned in a Gaussian fashion so that destructive interference causes the wake function to decrease rapidly and smoothly. Moderate damping provided by four waveguide manifolds running along the outer wall of the accelerator is utilised to suppress the reappearance of the wake function at long ranges where the interference becomes constructive again. The newly developed spectral function method, involving a continuum of frequencies, is applied to analyze the wake function of the DDS 1 design and to study the dependence of the wake function on manifold termination. The wake function obtained with the actually realized manifold terminations is presented and compared to wake function measurements recently carried out at the ASSET facility installed in the SLAC LINAC.

Paper presented at the 7th Workshop on Advanced Accelerator Concepts, Lake Tahoe, CA, October 13th-19th 1996

[1] Supported by Department of Energy grant number DE-FG03-93ER40759[‡] and DE-AC03-76SF00515[†]

DISCLAIMER

Analysis And Application Of Manifold Radiation In DDS 1: First Experiences

R.M. Jones[†‡], N.M. Kroll[†‡], M. Seidel[†], C. Adolphsen[†],
K.L.F. Bane[†], W.R.Fowkes[†], K. Ko[†],
R.H. Miller[†], R.D. Ruth[†], and J.W. Wang[†]

†*Stanford Linear Accelerator Center,*
Stanford University, Stanford, CA 94309
‡*University of California, San Diego,*
La Jolla, CA 92093-0319

Abstract. The frequency spectrum of the manifold radiation resulting from a uniformly displaced drive beam in DDS 1 has been calculated utilising the spectral function theory and compared with observations in the ASSET experiment. They are found to be in good qualitative agreement. The bulk of the radiation, both measured and computed, is found to emerge from the downstream end of the manifolds. This is in conflict with perturbation theory predictions, and is thus one more indication of the unreliability of perturbation theory for estimating manifold effects for DDS 1. Beam centering as a function of frequency is accomplished by minimizing manifold radiation within a narrow frequency band. This procedure provides information on structure misalignment. While misalignments in DDS 1 degraded the precision of beam centering which could be achieved by minimizing manifold radiation, the results obtained are considered to be encouraging.

1. INTRODUCTION

The damping manifolds of the SLAC Damped Detuned Structure (DDS) (1) are intended to perform two functions in addition to the damping of the long range wakefield. One is to facilitate pumping and the other is to provide information about alignment and beam position by monitoring the radiation which emerges from them. This paper is devoted to preliminary results obtained in connection with the latter function. In the next (second) section we discuss the equivalent circuit theory of manifold radiation and compare the results with microwave measurements carried out during the ASSET experiment. In the third section we discuss the use of manifold radiation to detect structure misalignment and to adjust beam parameters so as to minimize the transverse wake.

2. EQUIVALENT CIRCUIT THEORY CALCULATION OF MANIFOLD RADIATION

The equivalent circuit used to discuss the DDS consists of a sequence of sections each one of which corresponds to a cell and its contiguous section of manifold. For the purpose of discussion we write the equations in matrix form as follows:

$$\begin{pmatrix} \hat{H} & H_x^t \\ H_x & H - GR^{-1}G \end{pmatrix} \begin{pmatrix} \hat{a} \\ a \end{pmatrix} - f^{-2} \begin{pmatrix} \hat{a} \\ a \end{pmatrix} = f^{-2} \begin{pmatrix} xB \\ 0 \end{pmatrix} \tag{2.1}$$

Each component of the column matrices is an N component vector with â and a representing the TM and TE components of the cell excitation respectively. The square matrix on the right is a symmetric 2N by 2N matrix requiring nine circuit parameters per section for its description and whose elements are themselves N by N matrices. The N component column vector B on the RHS represents the coupling of the beam to the manifold. It is generally referred to as the cell kick factor and is normally defined "per unit beam displacement". Since we wish to consider cell dependent displacements we have represented the beam displacement at the n'th cell by the n'th diagonal element of the diagonal N by N matrix x. For all of the applications considered here the number of sections N is 206. For further details of the circuit model see (1) and (2).

In order to compute the power spectrum emerging from the manifolds we must first determine the manifold amplitude vector A defined in (2). We compute this quantity as follows: The TE amplitude vector a is obtained by solving Eq. 2.1 for the amplitude vectors in terms of the source vector xB (to which it is evidently linearly related.) A is in turn linearly related to a via the relation (2):

$$A = R^{-1}a \tag{2.2}$$

and thus also to xB. What is actually measured is the power spectrum bled off from the output of the manifolds. One can show (3) that the power spectrum of the radiation emerging from the manifolds is given by:

$$P = (q\delta x)^2 L F_p \frac{f}{2\pi} \mathrm{Sin}\phi A^{\dagger} A \tag{2.3}$$

where ϕ is the manifold phase advance function, L the structure length, δx the beam offset, q the beam charge, F_p the pulse repetition rate and f the frequency component. This quantity, eqn (2.3), is shown in Fig. 1, both for a uniform offset of 1.3 mm for all cells and for a uniform displacement of 1.3 mm confined to cells 19 to 186. The uniform offset curves are in good qualitative agreement with

the measurements and exhibit the large asymmetry observed between the upstream and downstream radiation. The sharp fall-offs in the spectra due to the limited range displacement as well as the fact that the central amplitudes for the full and limited range spectra are identical demonstrates a local or quasi local character of the excitation. The synchronous frequencies of cells 19 and 186 are 14.52 GHz and 15.55 GHz respectively and are identified by the dashed vertical lines in Fig. We estimate form Fig. 1. that the excitation frequency is shifted upward from the synchronous frequency by approximately 40 MHz at cell 19 and approximately 100 MHz at cell 186.

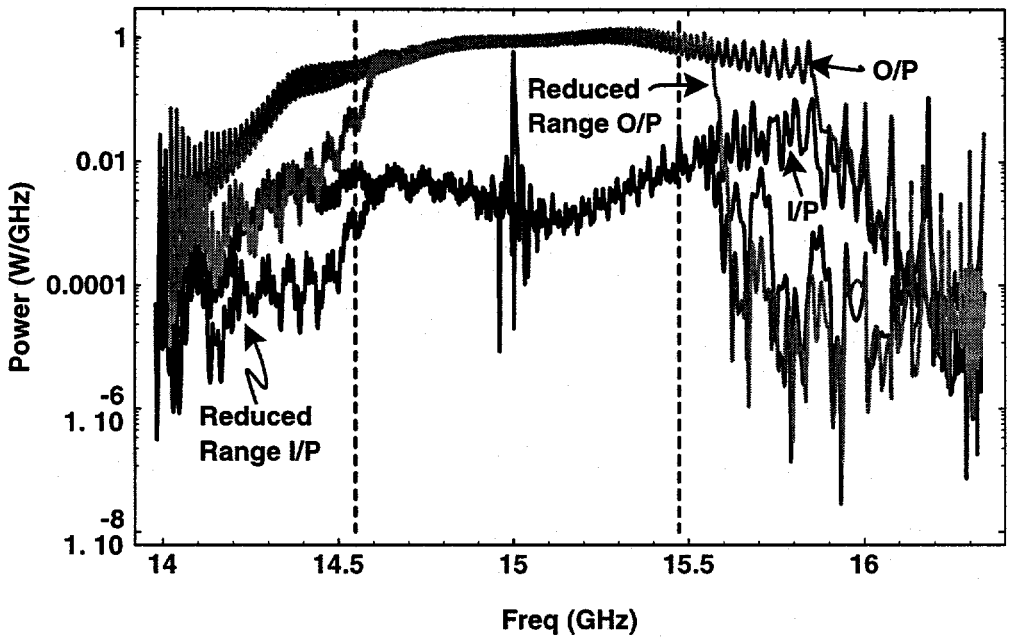

FIGURE 1. Power spectrum generated by a uniformly displaced beam calculated for the manifold input and output HOM couplers. Also shown are the corresponding power spectra when the displacement is limited to cells 19 to 186.

It appears from an examination of the modes themselves that excitation is occurring in the synchronous region of the modes, but that the synchronous points of the detuned modes are shifted from the cells whose synchronous frequency equals the mode frequency. As we shall see in the next section, a localized connection between frequency and excitation point has important practical consequences. The results obtained so far provide strong evidence that such a connection exists and indicate that the methodology applied above can determine it throughout the structure. It appears, however, that there will be a significant shift from the localization relation obtained from the cell synchronous frequencies. Another issue that we plan to investigate is the connection between the width of the localized displacement region and the frequency width of the power spectrum it generates.

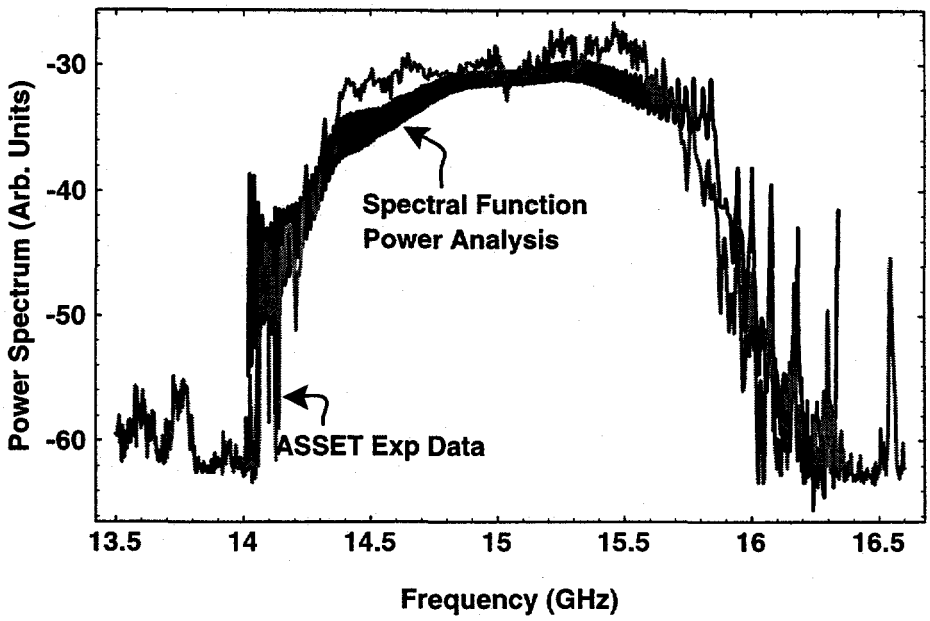

FIGURE 2. Computed and measured downstream power spectra compared for a uniformly displaced beam. Relative amplitudes (comparable absolute values are not known) are adjusted to facilitate comparison.

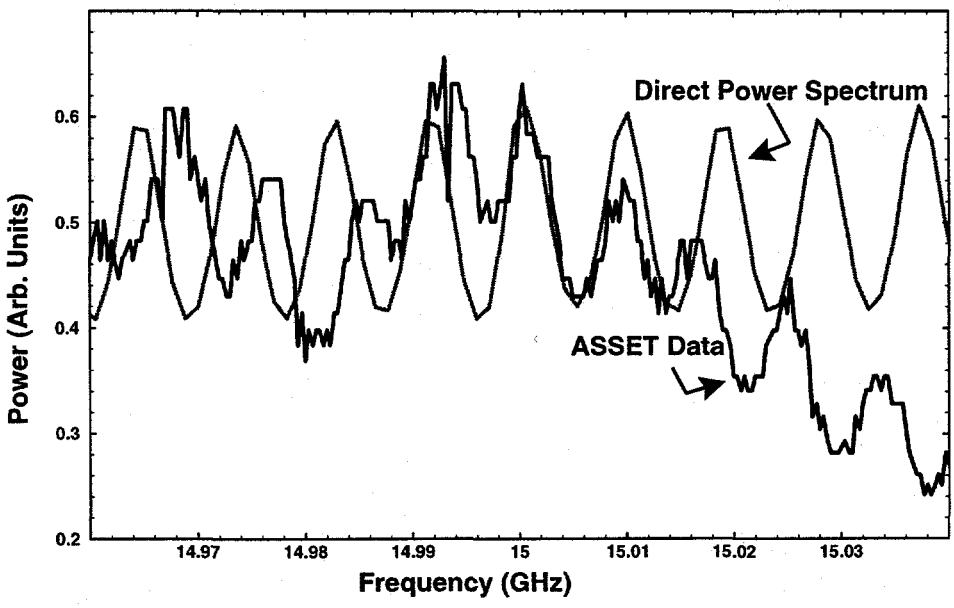

FIGURE 3. Computed and measured downstream power spectra for a uniformly displaced beam compared over a limited frequency band. A 1 MHz spectrum analyzer bandwidth setting facilitates comparison of the oscillatory structure.

Figure 3 shows a comparison between the computed and observed power spectrum (measured a 1 MHz bandwidth) in the region where maximum mode density is expected. One notes that the mean separation of the oscillatory peaks in the observed spectrum is approximately 10% less than that in the computed one. This result can be related to a discrepancy between the observed and computed wakes (ref (1) Fig. 6). Due to the mismatch, the computed wake shows a notable reappearance peak at a distance of 33 m. This reappearance peak was also observed in the measurements but at 36 m. The distance at which this peak is expected is given by c/df where df is a mean minimum mode separation. This relation implies 8.8 mode spacings for the computed manifold spectrum and 9.6 for the observed one in the 0.8 GHz frequency interval covered in the Fig. 3 curves.

3. APPLICATION OF MANIFOLD RADIATION TO THE DETECTION OF STRUCTURE MISALIGNMENT AND TO BEAM POSITION MONITORING

A principle objective of the study of manifold radiation was to determine how well one could minimize the wake by minimizing manifold radiation, and the precision to which one could center the beam in the structure. Unfortunately, a minor accident occurred during the assembly of DDS 1 which resulted in significant misalignment within the structure. This compromised to some extent the wake minimization program, but it provided an opportunity to observe the effect of misalignment on manifold radiation.

Instead of varying the beam offset to minimize total manifold power one can vary the beam offset to minimize manifold power at a particular frequency, thus determining a power minimizing offset $x_0(f)$ as a function of frequency as reported in (4). Mechanical measurement of the misalignment of DDS 1 as a function of cell number provided the opportunity to predict $x_0(f)$ from Eq. (2.2). For this purpose we assume that eqn. (2.1) still holds if the n'th element x_n of the diagonal offset matrix x is written $x_n = X_n + x_0(f)$, where X_n represents the mechanically measured cell offset. Then writing eqn (2.1) in the schematic form

$$P(f) = \sum_{m,n} M_m^*(f) M_n(f) (X_m + x_0(f))(X_n + x_0(f)) \tag{3.1}$$

one easily sees that P(f) is minimized if

$$x_0(f) = -\sum_{m,n} \mathrm{Re}\{M_m^*(f) M_n(f)\} X_n \Big/ \sum_{m,n} M_m^*(f) M_n(f) \tag{3.2}$$

The experimentally determined and computed $x_0(f)$ are compared in Fig. (4), showing good qualitative agreement. In an attempt to visually relate the mechanical offset data to the computed $x_0(f)$, we plot $-x_0(f_n)$ and the mechanical offset as a function of cell number n in Fig. (5). Here, as suggested by the quasi-locality noted in the previous section, we take fn = fsn + Cn, where f_{sn} is the synchronous frequency of the n'th cell and the constant C is chosen to yield the frequency shifts at cells 19 and 186 previously noted. The agreement is seen to be quite satisfactory. In connection with the poorer agreement shown in Fig. 4 it should be noted that there is some evidence based upon measurements performed at different times that the mechanical offsets shifted in the handling of the structure, so that there is some possibility that the mechanical offsets were different from those shown in Fig. 5 when the Fig. 4 measurements were made. Be that as it may, the gross feature of the mechanical measurement, the 60 μm shift at cell 45, was a constant feature of the measurements and is clearly echoed in both the measured and computed values of $x_0(f)$.

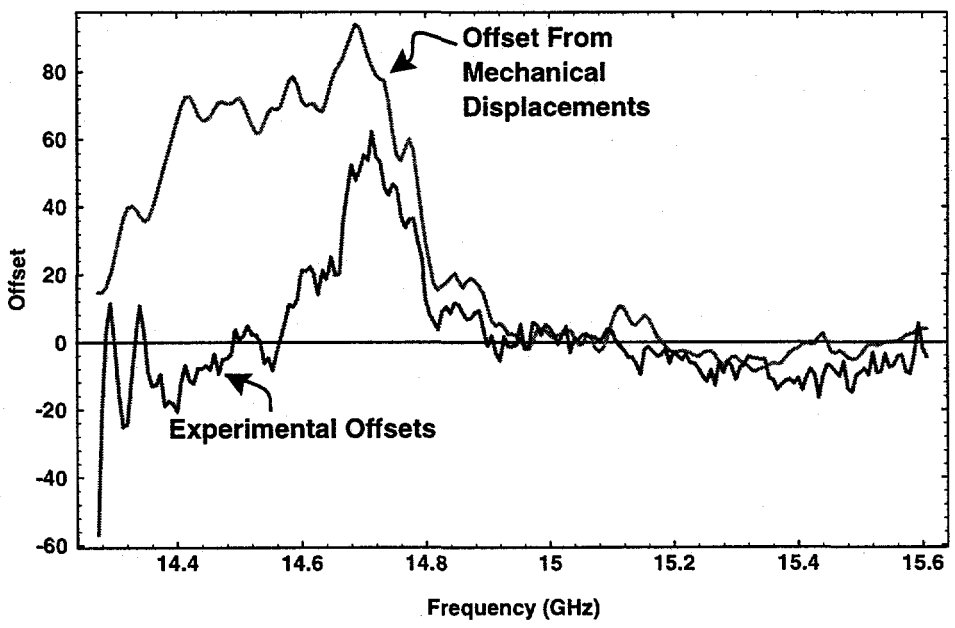

FIGURE 4:. Comparison of measured and computed manifold power spectrum minimizing offsets as a function of frequency.

Given the misalignment discussed above, there is clearly no beam position which zero's the manifold radiation at all frequencies. A number of techniques and criteria that one can use to fix the beam position are discussed in (4) and will not be repeated here. Analysis of the measured residual wake associated with these criteria is in progress and will be reported elsewhere. Because the residual wakes

are small, measurements are confined to the wake at short distances, before destructive interference has developed. It is a straightforward matter to compute this wake for the measured offsets and determine the compensating offset needed to negate it. The manifold spectrum associated with this arrangement can also be computed. Such computations may assist in developing beam positioning criteria for minimizing or zeroing the wake.

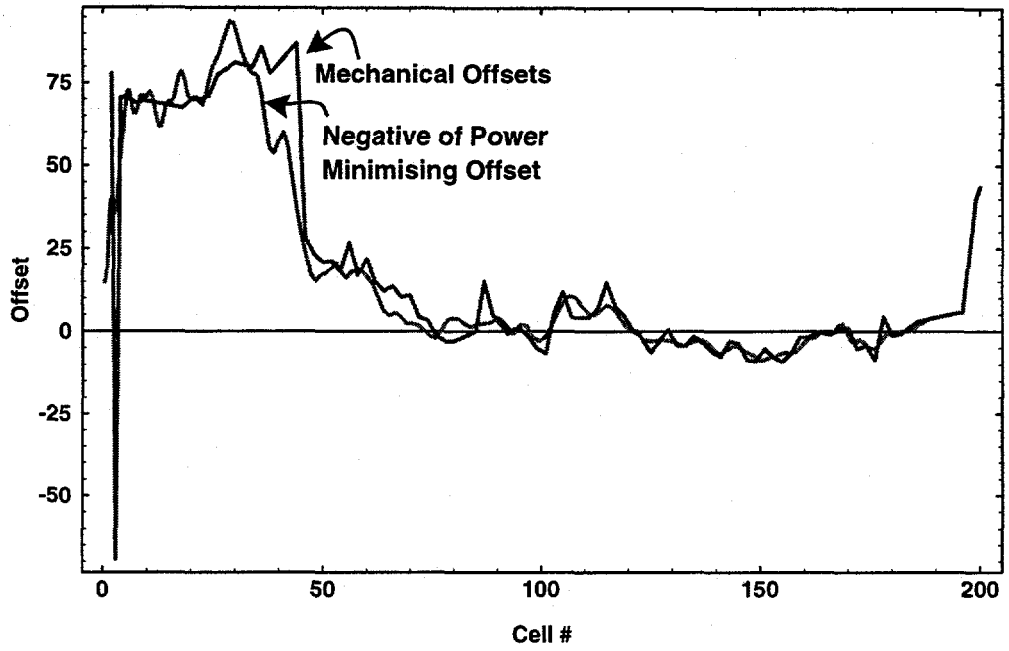

FIGURE 5. Mechanically measured offsets as a function of cell number. The computed power minimizing offsets at a set of cell associated frequencies (as described in the text) are also plotted for comparison.

4. ACKNOWLEDGEMENTS

This work is supported by Department of Energy grant number DE-FG03-93ER40759[‡] and DE-AC03-76SF00515[†]. We have benefited greatly from discussions at the weekly structures meeting at SLAC, where these results were first presented and thank all members of the group.

5. REFERENCES

1 Jones, R.M., Kroll, N.M, Adolphsen, C., Bane, K.L.F., Fowkes, W.R., Ko, K, Miller, R.H., Ruth, R.D, Seidel, M. and. Wang, J.W, "Recent Results & Plans For The Future On SLAC Damped Detuned Structures (DDS)". This issue; also SLAC-Pub-7387

2 Jones, R.M., Ko, K., Kroll, N.M. , Miller, R.H., & Thompson, K.A, "Equivalent Circuit Analysis of the SLAC Damped Detuned Structure", EPAC96, Sitges, Spain, June 10-14, 1996; SLAC-PUB-7187 (http://libnext.slac.stanford.edu/slacpubs/7000/slac-pub-7187.ps.Z)

3 Jones, R.M., Kroll, N.M. & Miller R.H., To be submitted to *Phys. Rev. E*, 1997
4. Seidel, M., et al, "Microwave Analysis of the Damped Detuned Accelerator Structure" , Linac96, Geneva, Switzerland,, 1996; SLAC-PUB-7289